EPJ Web of Conferences **93**, 01040 (2015)
DOI: 10.1051/epjconf/20159301040

Investigation of dipole strength up to the neutron separation energy at γELBE

R. Massarczyk[1,2,a], R. Schwengner[2], D. Bemmerer[2], R. Beyer[1,2], R. Hannaske[1,2], A. R. Junghans[2], M. Kempe[1,2], T. Kögler[1,2], G. Schramm[1,2], and A. Wagner[2]

[1] *Helmholtz-Zentrum Dresden-Rossendorf, 01328 Dresden, Germany*
[2] *Technische Universität Dresden, 01062 Dresden, Germany*

Abstract. The bremsstrahlung facility at the ELBE accelerator offers the possibility to investigate dipole strength distributions up to the neutron-separation energies with photon up to 16 MeV in energy. The facility and various results for nuclides measured during recent years are presented. One example is the study of the $N = 80$ nuclide ^{136}Ba. The other presented example is the study of the chain of xenon isotopes from $N = 70$ to $N = 80$ which aimed to investigate the influence of nuclear deformation an neutron excess on the dipole strength in the pygmy region. An overview of the analysis is given. GEANT4 simulations were performed to determine the non-nuclear background that has to be removed from the measured spectra. This opens up the possibility to take into account also the strength of unresolved transitions. Simulations of gamma-ray cascades were carried out that consider the transitions from states in the quasi-continuum and allow us to estimate their branching ratios. As a result, the photoabsorption cross sections obtained from corrected intensities of ground-state transitions are compared with theoretical predictions and results within the chain of isotopes. With the help of the measured dipole distribution it is possible to describe gamma-ray spectra following neutron capture more precisely.

1 Introduction

The strength function f and the nuclear level density ϱ can be used to describe the average transition width for the transition from an excited state i to another state f with the transition energy E_γ [1] :

$$\left\langle \Gamma_{if}^{XL} \right\rangle = \frac{f_{if}^{XL}(E_\gamma) \cdot E_\gamma^{2L+1}}{\varrho(E_i)}, \qquad (1)$$

Especially for the nuclear states excited in neutron, proton or α capture, which are relevant in astrophysical scenarios, the shape of the deexcitation spectrum and therefore, the photon energy distribution and multiplicity can be described with Eq. 1. Deexcitations to states lower than the excitation energy E_i are possible. The strength function is assumed to depend only on the transition energy $E_\gamma = E_i - E_f$ [2, 3] and the spins of the involved states. Therefore, also the distribution of the strength at lower energies is needed to describe the deexcitation probability correctly. The strength function can be split into contributions of different multipole orders and types. The electric dipole ($E1$) and magnetic dipole ($M1$) strength function are the dominating ones while higher orders are weaker. The photoabsorption cross section σ_γ is directly proportional to the strength function and therefore a suitable tool to investigate the distribution.

$$\left\langle \sigma_\gamma \right\rangle = 3\,(\pi\hbar c)^2\, E_\gamma f_{E1}(E_\gamma) \qquad (2)$$

Reaction cross sections for the (γ, n) process are measured for various nuclei above the neutron separation threshold. The characteristic bump of the giant dipole resonance (GDR) is seen at excitation energies around $E_x =$ 15 to 20 MeV in medium-mass nuclei. The shape can be fitted with a number of Lorentzian functions taking into account triaxial deformation of the nucleus [4, 5]. For simulations of reactions which occur in network calculations in nuclear astrophysics and nuclear safety, the low-energy tail of the GDR is often assumed to be just the extension of the Lorentzian-shaped bump. Detailed studies at the ELBE facility [6–13] and other facilities [14–19] have been performed during the last decade in order to learn and understand the behavior of the strength function below the neutron threshold. Additional resonances such as the so-called pygmy dipole resonance have been found in some nuclei to increase the strength. Their behavior with changing nuclear properties is quite unexplored and one of the main drivers in the research field of nuclear resonance fluorescence experiments nowadays [17].

2 Experimental facility

The γELBE facility [20] allows experiments with bremsstrahlung of maximum energies up to $E_\gamma \approx 15$ MeV. The electrons hit a thin niobium foil and are guided afterwards into a beam dump. Within the produced bremsstrahlung distribution the ratio of low-energy photons to high-energy photons is reduced by an aluminum-made beam hardener. The beam is shaped by a collimator

[a] e-mail: r.massarczyk@hzdr.de

in the wall and used in the experimental cave for scattering experiments. The electron energies of the ELBE accelerator can be adapted to the experimental needs. Usually the electron energy is chosen to be $E_{e^-} > S_n$ which ensures a continuously high photon flux up to the neutron separation thresholds, cf. Fig. 1.

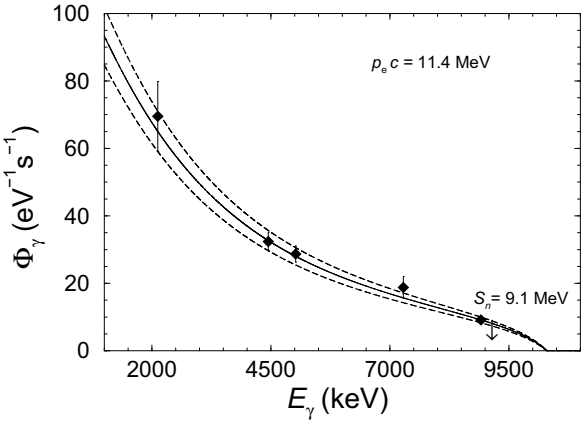

Figure 1. Photon flux distribution in a measurement on ^{136}Ba [9].

After photon irradiation of highly enriched targets the scattered photons are detected in high-purity Germanium (HPGe) detectors. Each detector is surrounded by a bismuth germanate scintillation detector. With this additional veto detector it is possible to reduce the amount of photons in the spectrum that have not depleted their full energy in the detector.

3 Results

3.1 Photoabsorption cross sections

To get the full information from the experimental data, we perform the following steps in the data analysis:

- Unfolding of detector response and efficiency using GEANT4 [21].
- GEANT4 is also used to determine the amount of non-nuclear events in the spectrum.
- The γDEX [7] code is used to remove events in the spectrum caused by inelastic scattering. The remaining spectrum is corrected for the ground-state branching ratios.

The final result of the data unfolding are results as shown in Fig. 2. Here, the average photoabsorption cross section in ^{136}Ba below the neutron separation energy is shown [9]. The result from γELBE is compared with the experimental result in the neighboring even-even isotope ^{138}Ba [22] was investigated at the HIγS facility with quasi-monoenergetic γ-ray beams. As one can see, the steps just mentioned are suitable for unfolding a measured broad-band spectrum and getting the full information. Hence, the results from ELBE are comparable with the results obtained with a quasi-monoenergetic beam.

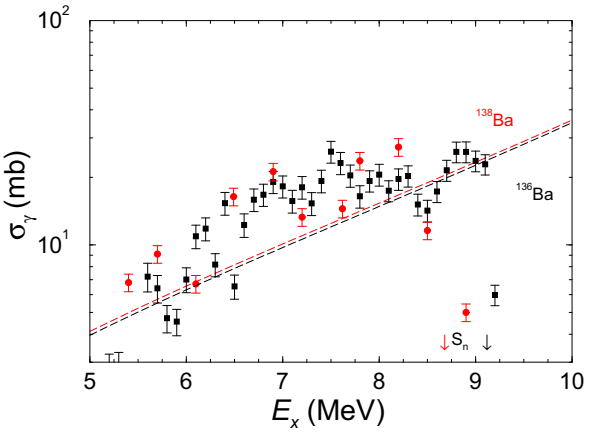

Figure 2. Comparison of photoabsorption cross sections from γELBE on ^{136}Ba [9] and from HIγS on ^{138}Ba [22].

3.2 Investigation of the behavior of the strength in the pygmy region

One of the major questions concerning the distribution of dipole strength at low excitation energies is the existence of so-called pygmy dipole strength [17]. This term is often used for the additional strength over the tail of a Lorentzian shaped giant dipole resonance. It is assumed that this additional strength depends on crucial parameters such as neutron excess. Therefore, a series of experiments in the isotope chains of molybdenum [11] and xenon [13] as well as in $N = 50$ isotones [6] has been performed at the γELBE facility.

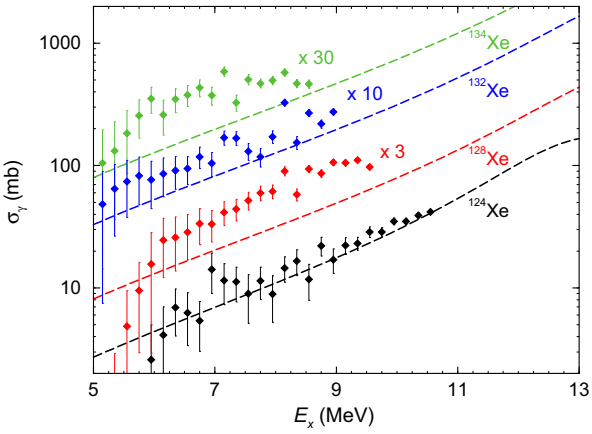

Figure 3. Photoabsorption cross sections for various xenon isotopes measured at ELBE [13] (colored data points). The dashed lines show the predictions of the TLO model.

Fig. 3 shows that within the xenon series, isotopes with larger neutron excess and therefore higher neutron-to-proton ratio show an increased cross section over the prediction of a triple-Lorentzian model (TLO,[5]). As no difference between tail of the GDR and additional strength can be done experimentally, often the full strength in a spe-

cific interval below the (γ,n) threshold is compared to the strength of the neighboring isotopes.

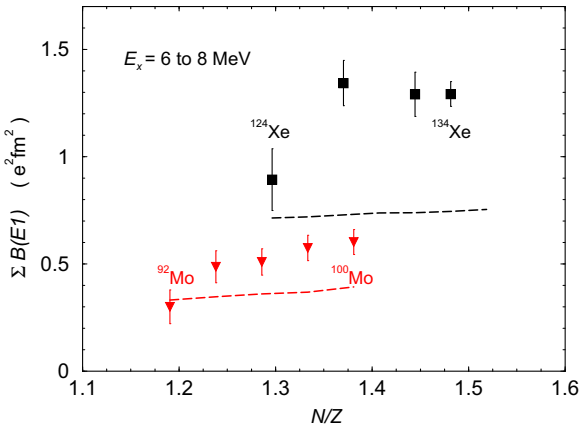

Figure 4. Cross section data taken from Ref.[13] and Ref.[11] and transformed into $B(E1)$ values. The measurement series in molybdenum and xenon isotopes (data points) are compared with predictions of the TLO-model (dashed lines).

In Fig. 4 the cross sections are transformed into $B(E1)$ values and summed up. What one can see for the two series of measurements is that the trend of increasing strength with increasing neutron excess as predicted by theory can be found also in the experiment. Additional studies have shown that the deformation which has a large impact on the shape of the giant resonance around its maximum has only smaller impact on the tail of the resonance [13].

3.3 Impact of the experimental deduced strengths on other reactions

We have studied the impact of experimental findings so far by the two following methods:

- **Implementation of experimentally deduced dipole strength in TALYS**
  For selected nuclei such as ^{139}La [23] and ^{181}Ta [24] the dipole strength has been determined and the experimental distribution implemented in the TALYS code [25]. The impact for neutron capture cross section at energies relevant for nuclear astrophysics has been studied and significant differences to model predictions have been found. The photon strength function in the neighboring isotope can have significant influence on the neutron capture cross section and can help to explain the abundances of isotopes at astrophysical branching points.
- **Combined data analysis of (γ,γ) and (n,γ) experiments**
  For the isotopes ^{78}Se [7], ^{196}Pt [8], and ^{114}Cd [26] the same kind of continuum analysis has been performed to combine the experimental strength function distributions with existing level densities. By using the code γDEX, it is possible to describe the photon spectrum after neutron capture. This distribution of photons which follow the decay of an excited state is an information which is needed also in the data analysis of photon-scattering experiments. A new model for the distribution of magnetic dipole strength [7] is used and it can be shown that the description of the γ cascade in the deexcitation of a resonant state after neutron capture is improved if one uses the experimental strength.

4 Summary

At γELBE one can measure photo-absorption cross sections with a high photon flux up to the neutron-separation energy. The usage of modern simulation-based analyzing methods allows the determination of the cross sections, especially in the region of the quasi-continuum of unresolvable states. The characteristics of the strength in the pygmy resonance region have been studied and it has been found that the strength in general dependends on the neutron excess of a nucleus. In addition, the experimental findings have been used to describe the observation in other experiments. Further, the impact of cross sections on network calculations relevant for astrophysics and on nuclear technology was investigated.

The work at γELBE has been supported by the German Research Foundation (DFG), project no. SCHW883/1-1 and partly by the EURATOM FP7 Project ERINDA (FP7-269499).

References

[1] G. Bartholomew *et al.*, Advances in Nuclear Physics **7** 229 (1973)
[2] D. Brink, PhD thesis, University of Oxford (1955)
[3] P. Axel, Phys. Rev. **126**, 671 (1962)
[4] R. Capote *et al.*, Nuclear Data Sheets **110**, 3107 (2009)
[5] A.R. Junghans *et al.*, Phys. Lett. B **670**, 200 (2008)
[6] R. Schwengner *et al.*, Phys. Rev. C **87**, 024306 (2013)
[7] G. Schramm *et al.*, Phys. Rev. C **85**, 014311 (2012)
[8] R. Massarczyk *et al.*, Phys. Rev. C **87**, 044306 (2013)
[9] R. Massarczyk *et al.*, Phys. Rev. C **86**, 014319 (2012)
[10] A. Makinaga *et al.*, Phys. Rev. C **82**, 024314 (2010)
[11] G. Rusev *et al.*, Phys. Rev. C **79** 061302(R) (2009)
[12] R. Schwengner *et al.*, Phys. Rev. C **78**, 064314 (2008)
[13] R. Massarczyk *et al.*, Phys. Rev. Lett. **112**, 072501 (2014)
[14] D. Savran *et al.*, Phys. Rev. Lett. **100**, 232501 (2008)
[15] D. Savran *et al.*, Phys. Rev. Lett. **97**, 172502 (2006)
[16] A. Zilges *et al.*, Phys. Lett. B **542**, 43 (2002)
[17] D. Savran *et al.*, Prog. Part. Nucl. Phys. **70**, 210 (2013)
[18] A.C. Larsen *et al.*, Phys. Rev. C **87**, 014319 (2013)
[19] M. Guttormsen *et al.*, Phys. Rev. Lett. **109**, 162503 (2012)

[20] R. Schwengner *et al.*, Nucl. Instr. Meth. A **555**, 211 (2005)
[21] S. Agostinelli *et al.*, Nucl. Instr. Meth. A **506**, 250 (2003)
[22] A. Tonchev *et al.*, Phys. Rev. Lett. **104**, 072501 (2010)
[23] M. Beard *et al.*, Phys. Rev. C **85**, 065808 (2012)
[24] A. Makinaga *et al.*, Phys. Rev. C **90**, 044301 (2014)
[25] A.J. Koning *et al.*, AIP Conf. Proc. 769, 1154 (2005)
[26] R. Massarczyk *et al.*, to be submitted